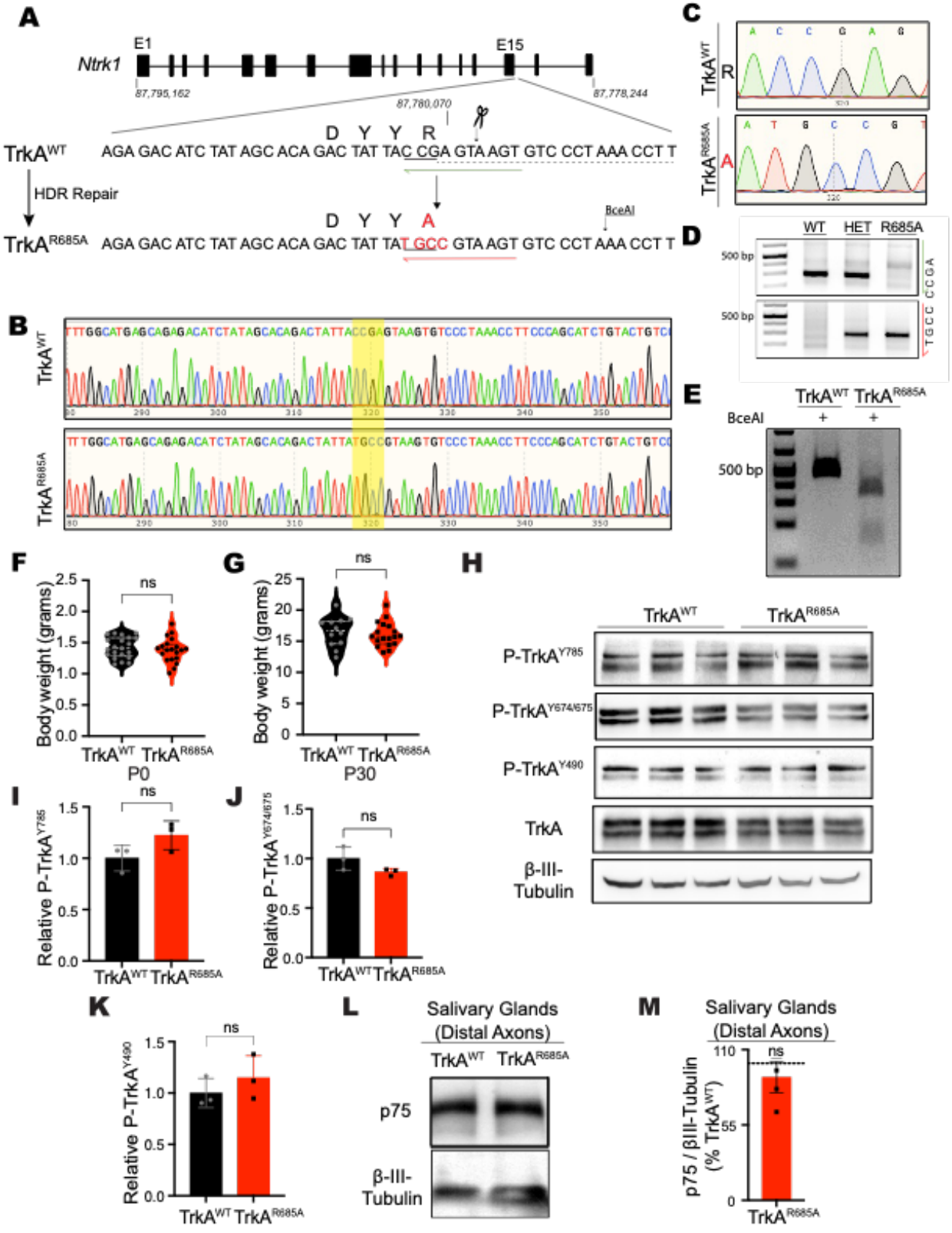

Supplemental Figure S1. Generation of TrkA^{R685A} knock-in mice. Related to Figure 1.

(A) Schematic for generation of TrkA^{R685A} knock-in mice. The top row shows the TrkA (*Ntrk1*) gene structure. The middle row shows the coding sequence for PTP1B interaction motif (DYYR) at exon 15 in the TrkA^{WT} allele and the Cas9 target region. Target sequence for gRNA is indicated by dashed underline, and the PAM site is indicated by solid underline. The bottom row shows the coding sequence in the TrkA^{R685A} allele after homology-directed repair (HDR). The altered nucleotide sequence, TGCC, and the corresponding amino acid, A, are shown in red. A silent C > T mutation destroys the original PAM sequence and creates a novel BceAI restriction site for Restriction fragment length polymorphism (RFLP) analysis. Green arrow (TrkA^{WT} allele) and red arrow (TrkA^{R685A} allele) indicate allele-specific primers for PCR genotyping. **(B)** PCR genotyping results. A common forward primer and allele-specific reverse primers result in a band of 287 bp for TrkA^{WT} and TrkA^{R685A}. **(C)** Identification of TrkA^{R685A} knock-in animals via RFLP analysis using BceAI restriction digest. TrkA^{WT} band size: 467 bp. TrkA^{R685A} band sizes: 367bp and 100bp. **(D)** Sanger-sequencing analysis of founder mice confirms genetic modification to TrkA^{R685A}. **(E)** Sequencing of TrkA^{WT} and TrkA^{R685A} alleles shows preservation of surrounding nucleotides. **(F, G)** TrkA^{R685A} animals have similar body weight as littermate controls at birth **(F)** and at postnatal day 30 **(G)**. ns=not significant, t-test. (**H)** Immunoblotting for P-TrkA^{Y785}, P-TrkA$^{Y674/Y675}$, P-TrkA^{Y490}, and total TrkA in SCG lysates prepared from P0 TrkA^{R685A} mice and littermate controls. Three replicates for each genotype are shown. P-TrkA blots were stripped and re-probed for TrkA and β-III-tubulin as loading control. (**I-K)** Densitometric quantification of P-TrkA^{Y785} **(I)**, P-TrkA$^{Y674/Y675}$ **(J)**, and P-TrkA^{Y490} **(K)** levels in TrkA^{R685A} and control mice, normalized to total TrkA. Results are means ± SEM from n=3 mice per genotype and expressed as fold-change relative to the TrkA^{WT} condition. ns= not significant, t-test. (**L)** p75 protein levels in salivary gland lysates from E16.5 TrkA^{R685A} embryos are unaltered compared to littermate controls. **(M)** Densitometric quantification of p75 protein level in salivary gland lysates normalized to β-III-tubulin. Results are

means ± SEM from n=3 mice per genotype. p75 expression in mutant axons is represented as a % of p75 protein levels in control lysates. One-sample t-test, n.s.= not significant.

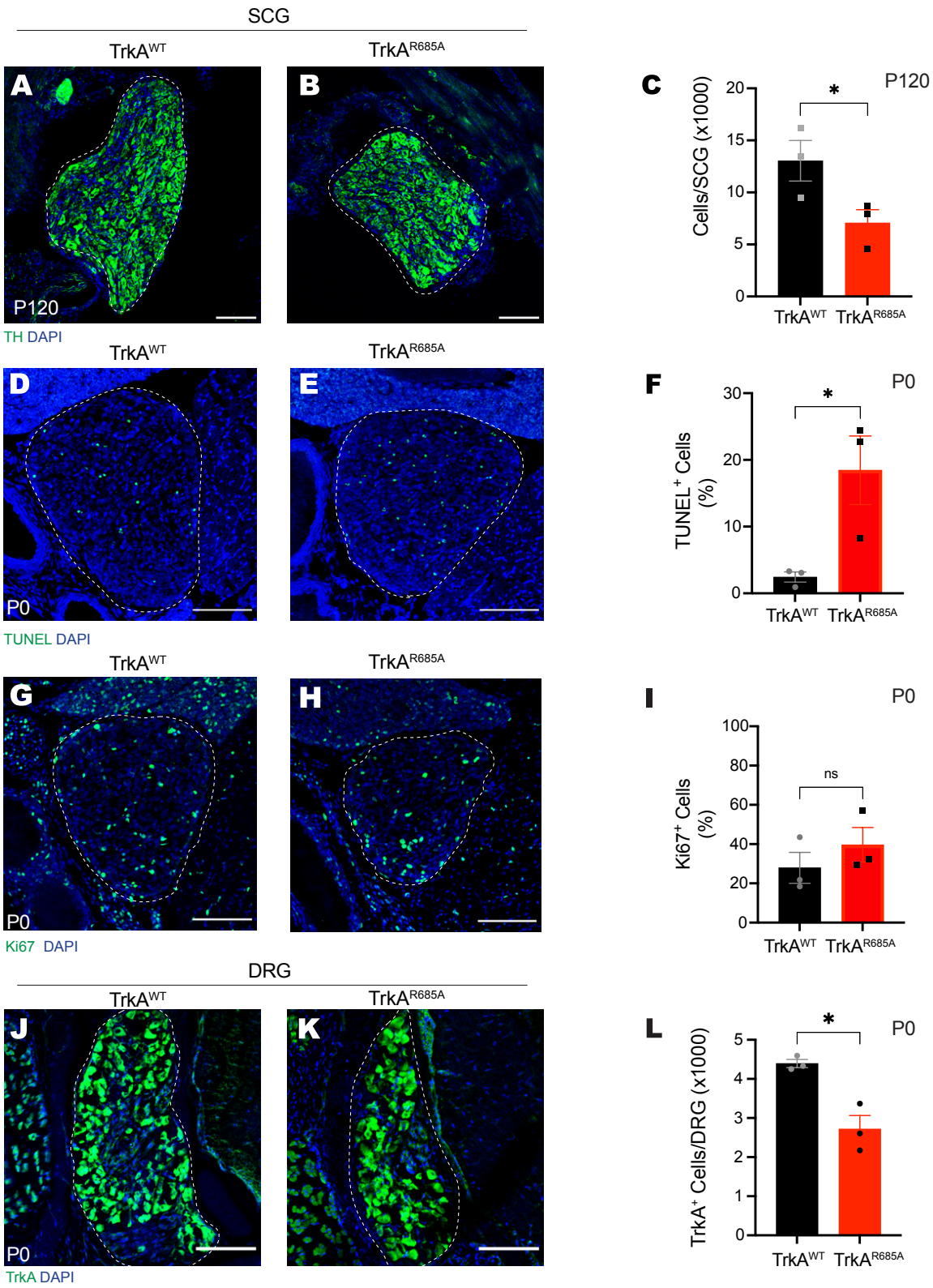
SCG
TrkA^WT
TrkA^R685A
A
B
P120
TH DAPI
TrkA^WT
TrkA^R685A
D
E
P0
TUNEL DAPI
TrkA^WT
TrkA^R685A
G
H
P0
Ki67 DAPI
DRG
TrkA^WT
TrkA^R685A
J
K
P0
TrkA DAPI
C
P120
Cells/SCG (x1000)
20
15
10
5
0
*
TrkA^WT
TrkA^R685A
F
P0
TUNEL+ Cells (%)
30
20
10
0
*
TrkA^WT
TrkA^R685A
I
P0
Ki67+ Cells (%)
100
80
60
40
20
0
ns
TrkA^WT
TrkA^R685A
L
P0
TrkA+ Cells/DRG (x1000)
5
4
3
2
1
0
*
TrkA^WT
TrkA^R685A

Supplemental Figure S2. Neuron survival defects in TrkA^{R685A} mice. Related to Figure 2.

(A-C) TH immunostaining, and cell counts performed on Nissl-stained SCG tissue sections, shows reduced sympathetic neuron number in 4-month old TrkA^{R685A} mice compared to litter-mate controls. Scale bar: 100 µm. Results are means ± SEM from n=3 mice per genotype, *p<0.05, t-test. **(D-F)** TUNEL labeling shows increased cell death in P0 TrkA^{R685A} SCGs compared to controls. Scale bar: 100 µm. Results are mean ± SEM from 3 mice per genotype and represented as % of TrkA^{WT} values, *p<0.05, t-test. **(G-I)** Cell proliferation is unaffected in P0 TrkA^{R685A} SCG compared to ganglia from littermate controls as assessed by Ki67 immunostaining. Scale bar: 100 µm. Results are mean ± SEM from 3 mice per genotype and represented as % of TrkA^{WT} values, *n.s: not significant, t-test. **(J-L)** TrkA-positive sensory neurons are significantly reduced in T13 DRG from P0 TrkA^{R685A} mice compared to litter-mate controls as assessed by TrkA immunostaining and neuronal counts. Nuclei are stained with DAPI (blue). Scale bar: 100 µm. Results are means ± SEM from n=3 mice per genotype, * p<0.05, t-test.

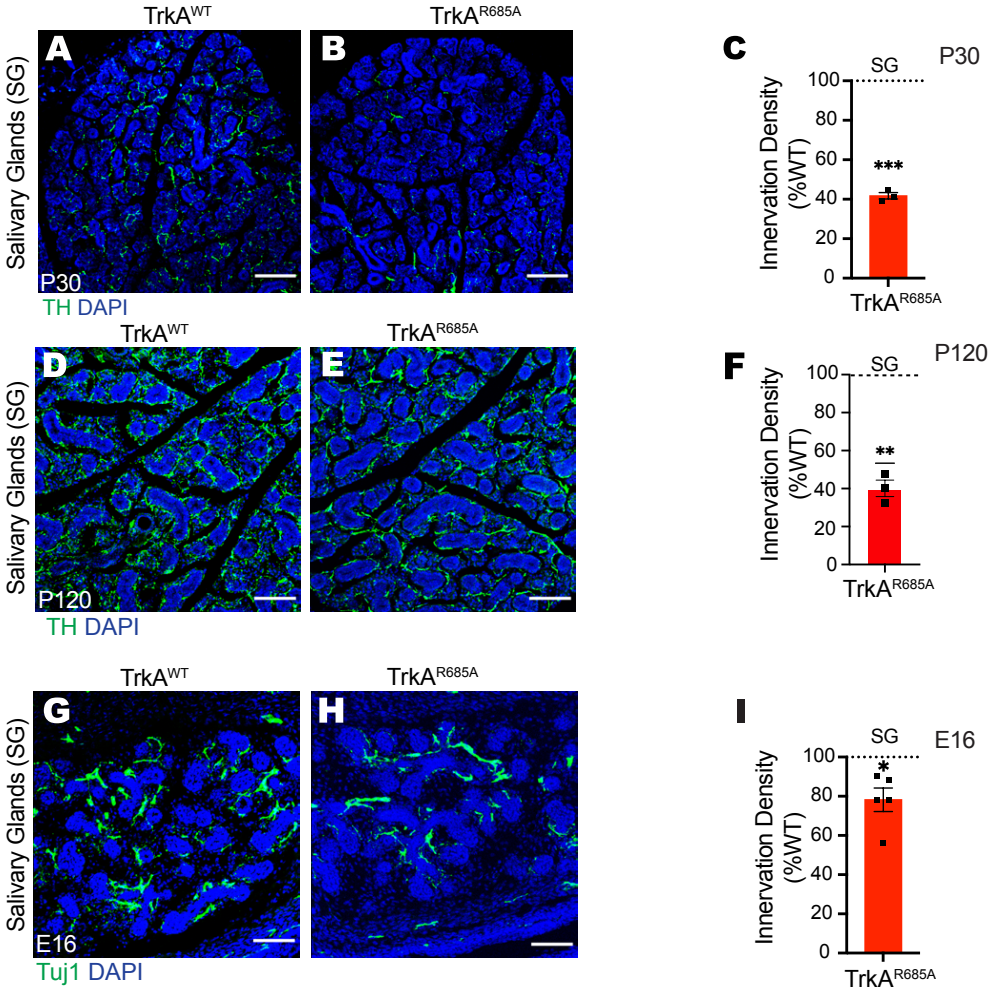
TrkA^WT
TrkA^R685A
A
B
Salivary Glands (SG)
P30
TH DAPI
C
P30
SG
Innervation Density (%WT)
100
80
60
40
20
0
***
TrkA^R685A
D
E
P120
F
P120
**
G
H
E16
Tuj1 DAPI
I
E16
*

Supplemental Figure S3. Sympathetic axon growth defects in TrkA^{R685A} mice. Related to Figure 3. (**A-C**) TH immunostaining of salivary glands and quantification of innervation density shows marked depletion of sympathetic innervation in P30 TrkA^{R685A} mice compared to litter-mate controls. Scale bar: 100 μm. **(D-F)** TH immunostaining and quantification of TH-positive nerves in salivary glands shows that the axon innervation deficit in 4-month old TrkA^{R685A} mutant mice is similar to that in 1-month old mice (**S3C**). Scale bar: 100 μm. (**G-I**) Immunostaining with a pan-neuronal marker, Tuj1, reveals a decrease in innervation in E16 salivary glands, compared to littermate controls. Nuclei are stained with DAPI (blue). Scale bar: 100 μm. **(C, F, I)** Quantification of TH-positive or Tuj1 positive nerves by measuring integrated fluorescence densities per unit area using ImageJ. Results are mean ± SEM from 3-4 mice per genotype and represented as % of TrkA^{WT} values. One-sample t-test with hypothetical mean of 100%; *p<0.05, **p<0.01, ***p<0.001.

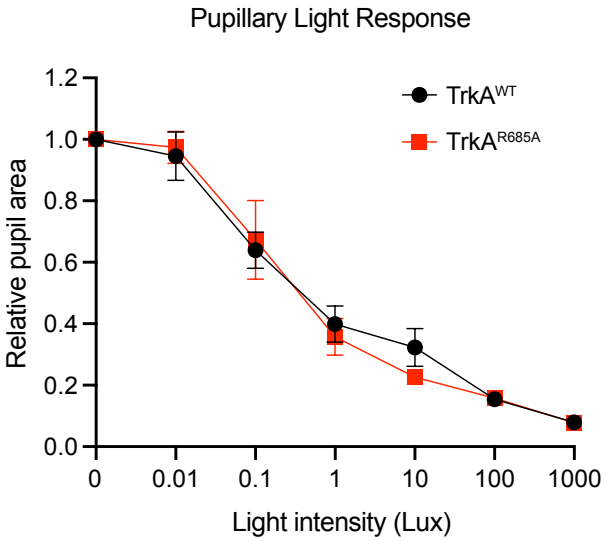
Pupillary Light Response
TrkA^WT
TrkA^R685A
Relative pupil area
1.2
1.0
0.8
0.6
0.4
0.2
0.0
0
0.01
0.1
1
10
100
1000
Light intensity (Lux)

Supplemental Figure S4. Autonomic function analysis. Related to Figure 5.

Parasympathetic activity is normal in TrkA^{R685A} mice as assessed by measuring pupil constriction in response to increasing light intensities. Data are mean ± SEM from n=6 TrkA^{WT} and 5 TrkA^{R685A} animals.

Supporting Information Materials and Methods:

Key Resources Table:

REAGENT or RESOURCE	SOURCE	IDENTIFIER
Antibodies		
Rabbit anti-P-TrkA^{Y785}	Cell signaling	Cat# 4168; RRID: AB_10620952
Rabbit anti-P-TrkA$^{Y674/675}$	Cell Signaling	Cat# 4621T; RRID: AB_916186
Rabbit anti-P-TrkA^{Y490}	Cell Signaling	Cat# 9141L; RRID: AB_2298805
Rabbit anti-P-Akt	Cell signaling	Cat# 9271; RRID: AB_329825
Mouse anti-P-Erk1/2	Cell signaling	Cat# 9106 RRID: AB_331768
Rabbit anti- p85 subunit of phosphatidylinositol-3-kinase	Millipore	Cat# ABS234; RRID: AB_2714180
Mouse anti-FLAG M2, IgG1	Sigma	Cat# F3165; RRID: AB_259529
Mouse anti-Trk (B-3)	Santa Cruz Biotechnology	Cat# sc-7268 RRID: AB_628397
Rabbit anti-TrkA	Millipore	Cat# 06-574; RRID: AB_310180
Mouse anti-β-III Tubulin (SDL.3D10), IgG2b	Sigma	Cat# T8660; RRID: AB_477590
Rabbit anti-TH	Millipore	Cat# AB152; RRID: AB_390204
Rabbit anti-Cleaved Caspase 3	Cell Signaling	Cat# 9661S; RRID: AB_2341188
Mouse anti-β-III Tubulin (Tuj1)	R & D Systems	Cat# MAB1195-SP RRID: AB_357520
Rat anti-Ki67 monoclonal (SolA15)	Thermo Fisher Scientific	Cat# 14-5698-82 RRID: AB_10854564
Mouse anti-p75	Biosensis	Cat# M-006-100 RRID: AB_2492395
Rabbit anti-NGF	Sigma	Cat# N6655; RRID: AB_477660
Sheep anti-NGF	Cedarlane	Cat# CLMCNET-031; RRID: AB_10060173
Amersham ECL Rabbit IgG, HRP-linked whole Ab (from donkey)	Cytvia Life Sciences	Cat# NA934-1ML; RRID:
Amersham ECL Mouse IgG, HRP-linked whole Ab (from sheep)	Cytvia Life Sciences	Cat# NA931-1ML; RRID:
Goat anti-Rabbit IgG (H+L) Highly Cross-Adsorbed Secondary Antibody, Alexa Fluor 488	Thermo Fisher Scientific	Cat# A-11034; RRID: AB_2576217
Goat anti-Mouse IgG2b Cross-Adsorbed Secondary Antibody, Alexa Fluor 546	Thermo Fisher Scientific	Cat# A-21143; RRID: AB_2535779
Goat anti-Mouse IgG1 Cross-Adsorbed Secondary Antibody, Alexa Fluor 546	Thermo Fisher Scientific	Cat# A-21123; RRID: AB_2535765
Bacterial and Virus Strains		
Adenovirus FLAG-TrkB:A^{F592A}-P2A-GFP (WT)	[1]	N/A

Adenovirus FLAG-TrkB:A$^{F592A/R685A}$-P2A-GFP (R685A)	[1]	N/A
	[2]	
Biological Samples		
NGF	[3]	N/A
Cas9	JHU Transgenic Core	N/A
Taq Polymerase	New England Biolabs	Cat# M0273
Chemicals, Peptides, and Recombinant Proteins		
BceAI Restriction Enzyme	New England Biolabs	Cat# R0623S
dNTP	Thermo Fisher Scientific	Cat# R0181
Collagenase Type II	Worthington	Cat#
Hyaluronidase		Cat#
DNaseI		Cat#
Bovine Serum Albumin		Cat#
Doxycycline hyclate	Sigma-Aldrich	Cat# D9891-5G
Cytosine β-D-arabinofuranoside hydrochloride	Sigma-Aldrich	Cat# C6645-5G
BDNF	PeproTech	Cat# 450-02
Protein G-Agarose Beads	Santa Cruz	Cat# sc-2002
Complete Mini, EDTA-Free	Roche	Cat# 11836170001
Pierce Phosphatase inhibitor Mini tablets	Thermo Fisher Scientific	Cat# A32957
Signal Enhancer HIKARI 250	Nacalai	Cat# NU00102
One Block Western-CL	Prometheus	Cat# 20-313
Dry Milk	Quality Biological	Cat# A614-1005
Restore PLUS Western Blot Stripping Buffer	Thermo Fisher Scientific	Cat# 46430
Pierce ECL Plus	Thermo Fisher Scientific	Cat# 32132
Cresyl Violet acetate	MilliporeSigma	Cat# C5042-10G
Gum Rosin	MilliporeSigma	Cat# 60895-1KG
boc-aspartyl(O-methyl)-fluoromethylketone (BAF)	BioVision	Cat# 1160-5
FluoSpheres™ Carboxylate-modified microspheres, 0.04µm (660/680)	ThermoFisher	Cat# F8789
DAPI	Roche	Cat# 10236276001
Critical Commercial Assays		
Adeno-XTM Adenoviral System 3 kit	Clontech	Cat# 631180
VivaPure AdenoPack20	Sartorius	Cat# VS-AVPQ020
PCR clean-up/ Gel extraction kit	Macherey-Nagel	Cat# 740609.250
In Situ Cell Death Detection Kit, Fluorescein	Millipore Sigma	Cat# 11684795910
Experimental Models: Cell Lines		
HEK 293	ATCC	CRL-1573
Experimental Models: Organisms/Strains		
TrkA^{R685A} knock-in mice	This paper	N/A
Sprague Dawley rats	Taconic Biosciences	SD-F

Oligonucleotides		
CRISPR guide RNA	This paper	N/A
CRISPR HDR Template	This paper	N/A
CRISPR transactivating RNA (tracr)	JHU Transgenic Core	N/A
$TrkA^{WT}$ -R: 5'- AGGTTTAGGGACACTTACTCGG -3'	This paper	N/A
$TrkA^{R685A}$-R: 5'- AGGTTTAGGGACACTTACGGCA -3'	This paper	N/A
$TrkA^{Common}$-F: 5'- TCTCTCTGTCTCCGTCTTTCT -3'	This paper	N/A
$TrkA^{R685A(BceA1)}$-F: 5'- CCTAGTCTCTTCCTTCCTCAAATC -3'	This paper	N/A
$TrkA^{R685A(BceA1)}$-R: 5'- CCAGAGCTCACACTGCTAAA -3'	This paper	N/A
Recombinant DNA		
N/A		
Hardware, Software and Algorithms		
Campenot Chambers	Tyler Research Corp.	Camp10
DESKGEN CRISPR, Desktop Genetics™	[4]	https://www.deskgen.com/guidebook
CHOP CHOP	[5]	https://chopchop.cbu.uib.no
Edit-R HDR Donor Designer software	Horizaon Discovery (Dharmacon)	https://horizondiscovery.com/en/ordering-and-calculation-tools/crispr-design-tool
Sony 20.6 Megapixel 4K HD Video Recording FDRAX33 Handycam Camcorder DCR-HC96	Amazon	N/A
EXTECH Foot Candle/Lux Light Meter	Grainger, Inc	Cat# 1H153
Sunlite A19 Light Bulb, Daylight	Amazon	N/A
Sunlite 80599-SU LED A19 Super Bright Light Bulb, Daylight	Amazon	N/A
Neutral Density Fillter (Roscolux)	Chesapeake Lighting	N/A
ZEN 2012 SP1 (black edition)	N/A	https://www.zeiss.com/microscopy/int/home.html
ZEN 2012 (blue edition)	N/A	https://www.zeiss.com/microscopy/int/home.html
ImageJ	N/A	https://imagej.nih.gov/ij/
Prism 9	GraphPad	https://www.graphpad.com/
Adobe Illustrator	Adobe	https://www.adobe.com

References:

1 Yamashita, N., Joshi, R., Zhang, S., Zhang, Z. Y. & Kuruvilla, R. Phospho-Regulation of Soma-to-Axon Transcytosis of Neurotrophin Receptors. *Developmental cell* **42**, 626-639 e625 (2017). https://doi.org:10.1016/j.devcel.2017.08.009

2 Ascano, M., Richmond, A., Borden, P. & Kuruvilla, R. Axonal targeting of Trk receptors via transcytosis regulates sensitivity to neurotrophin responses. *The Journal of neuroscience : the official journal of the Society for Neuroscience* **29**, 11674-11685 (2009). https://doi.org:10.1523/JNEUROSCI.1542-09.2009

3 Mobley, W. C., Schenker, A. & Shooter, E. M. Characterization and isolation of proteolytically modified nerve growth factor. *Biochem.* **15**, 5543-5551 (1976).

4 Hough, S. H., Ajetunmobi, A., Brody, L., Humphryes-Kirilov, N. & Perello, E. Desktop Genetics. *Per Med* **13**, 517-521 (2016). https://doi.org:10.2217/pme-2016-0068

5 Labun, K., Montague, T. G., Gagnon, J. A., Thyme, S. B. & Valen, E. CHOPCHOP v2: a web tool for the next generation of CRISPR genome engineering. *Nucleic Acids Res* **44**, W272-276 (2016). https://doi.org:10.1093/nar/gkw398